J. Fluid Mech. (2008), *vol.* 612, *pp.* 1–19.
doi:10.1017/S0022112008002619 Printed in the United Kingdom

Soret-driven thermosolutal convection induced by inclined thermal and solutal gradients in a shallow horizontal layer of a porous medium

P. A. LAKSHMI NARAYANA[1], P. V. S. N. MURTHY[1] AND RAMA SUBBA REDDY GORLA[2]†

[1]Department of Mathematics, Indian Institute of Technology, Kharagpur, Kharagpur – 721 302, W. B., India

[2]Department of Mechanical Engineering, Cleveland State University, Cleveland, OH 44115, USA
r.gorla@csuohio.edu

(Received 10 July 2007 and in revised form 21 May 2008)

The stability of Soret-driven thermosolutal convection in a shallow horizontal layer of a porous medium subjected to inclined thermal and solutal gradients of finite magnitude is investigated theoretically by means of a linear stability analysis. The horizontal components of these gradients induce a Hadley circulation, which becomes unstable when vertical components are sufficiently large. We employed a two-term Galerkin approximation for various modes of instability. The effect of the Soret parameter on the mechanism of instability of the thermosolutal convection is investigated. Results are presented for various values of the governing parameters of the flow. It is observed that the Soret parameter has a significant effect on convective instability and this is discussed.

1. Introduction

In this paper, we study the linear stability of a steady convective double diffusive flow of Hadley type considering the Soret effect which is set up by the horizontal components of temperature and concentration gradients in a shallow horizontal layer of a fluid-saturated porous medium. The instability arises as a result of the presence of a vertical component of the temperature gradient.

A large number of papers have been published dealing with natural convection in a horizontal layer, induced by either horizontal or vertical temperature gradients, but very few have dealt with the more general situation of inclined temperature gradients. Weber (1973) considered the problem of thermal convection with horizontal temperature gradients in a viscous fluid. Weber (1974) analysed the effect of horizontal and vertical thermal gradients on convection in a porous medium. Bhattacharrya & Nadoor (1976) analysed the stability of thermal convection between non-uniformly heated plates whereas Sarkar & Phillips (1992) analysed the effects of horizontal gradients on thermohaline instabilities in a thick porous layer. Parthiban & Patil (1993) studied the effect of inclined temperature gradient on thermal instability in an anisotropic porous medium. Parthiban & Patil (1994) analysed the effect of inclined gradients on thermohaline convection. Parthiban & Patil (1997) analysed the thermal

† Author to whom correspondence should be addressed.

instability in an anisotropic porous medium with internal heat source and inclined temperature gradient. Manole & Lage (1995) analysed the supercritical Hadley circulation within a porous layer, induced by an inclined temperature gradient. Also Manole, Lage & Antohe (1995) analysed the bifurcation to a travelling wave in a supercritical Hadley circulation within a layer of fluid-saturated porous medium. Manole, Lage & Nield (1994) studied the convection induced by inclined thermal and solutal gradients, with horizontal mass flow, in a shallow horizontal layer of a porous medium. Guo & Kaloni (1995) analysed the nonlinear stability of thermosolutal convection induced by inclined thermal and solutal gradients. Kaloni & Qiao (1997) studied the nonlinear stability of convection in a porous medium with inclined temperature gradient and extended their work to analyse the nonlinear convection in a porous medium with inclined temperature gradient and variable gravity field (Kaloni & Qiao 2001). Qiao & Kaloni (1997) studied the convection induced by inclined temperature gradient with mass flow in a porous medium. Convection induced by inclined gradients in a shallow porous medium layer has been discussed by Lage & Nield (1998). Qiao & Kaloni (1998) analysed the nonlinear convection in a porous medium with inclined temperature gradient. Thorpe, Hutt & Souloby (1973) studied the effect of horizontal gradients on thermohaline convection. Nield (1990) studied the problem of convection in a porous medium with inclined temperature gradient, and extended his work to study the effects of horizontal mass flow (Nield 1991) and additional results were presented in Nield (1994). Also Nield (1998) analysed the convection in a horizontal layer of porous medium with inclined temperature gradient considering vertical through flow. Alex & Patil (2001) analysed variable gravity effects on thermal instability in a porous medium with internal heat source and inclined temperature gradient, and extended their work to analyse variable gravity field on thermal instability in a porous medium with inclined temperature gradient and vertical through flow (Alex & Patil 2001). Alex & Patil (2002) studied the effect of variable gravity field on convection in an anisotropic porous medium with internal heat source and inclined temperature gradient. Nield, Manole & Lage (1993) analysed the thermosolutal convection in a horizontal layer of a porous medium with inclined temperature and concentration gradients. A review on convection with inclined temperature gradients can be found in Nield & Bejan (2006).

The terms Soret effect and Dufour coefficient give rise to interaction between the thermal and solute fields even when the fluid is at rest. However, it is well known that the Soret coefficient has a considerable effect on the convection process in liquids, whereas the literature survey reveals that the Dufour effect can be negligible in liquids, but it plays a prominent role in gaseous mixtures. Hurle & Jakeman (1971) have analysed theoretically the Soret effect on the Rayleigh–Jeffrey problem neglecting the Dufour coefficient and have shown that stable solutions could occur owing to this effect in water–methanol mixtures when they are heated from below. Eckert & Drake (1972) have analysed the effect of the Soret and Dufour parameters on convection heat and mass transport in the medium. Platten & Chavepeyer (1973) have analysed oscillatory motion in Bénard cells due to the Soret effect theoretically and experimentally. Thermosolutal convection in a solution with large negative Soret coefficient has been analysed by Caldwell (1976). Elementary transition state theory of the Soret and Dufour effect in ideal mixtures was discussed in Mortimer & Eyring (1980). Zimmermann, Muller & Davis (1992) analysed the Bénard convection in binary mixtures with the Soret effect and performed experiments on mixtures of ethyl alcohol and water. Bahloul, Boutana & Vasseur (2003) analysed the problem of double-diffusive and Soret-induced convection in a shallow horizontal porous layer analytically

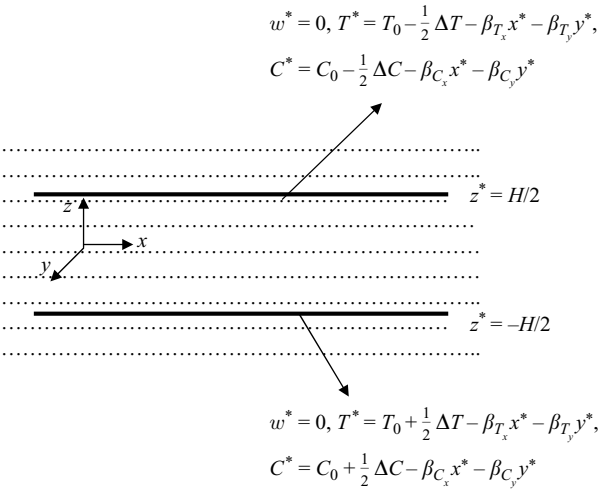

FIGURE 1. Schematic of the problem.

and numerically on a natural convection process filled with binary fluid under prescribed uniform heat and mass flux conditions on the boundaries. Alex, Patil & Venkatakrishnan (2001) analysed the effect of variable gravity field on thermosolutal convection in a porous medium considering the Soret effect. Thermodiffusion in porous media and its consequences are discussed in Costèque, Fargue & Janet (2002). Platten, Dutrieux & Chavepeyer (2002) presented techniques to measure the Soret effect on free convection. Platten *et al.* (2003) presented benchmark values for the Soret effect of three binary organic liquid mixtures. Delahaye, Bahloul & Vasseur (2002) studied the influence of the Soret effect on convection in a binary liquid layer with a free upper surface whereas Ouriemi, Vasseur & Bahloul (2005) analysed the natural convection of a binary mixture confined in a slightly inclined tall enclosure considering the Soret effect. Platten (2006) reviews experimental results for the Soret effect.

This study is an extension to Nield *et al.* (1993) by including the Soret effect in the medium. We incorporated the novel scaling given in Nield *et al.* (1993) such that the horizontal Rayleigh numbers appear explicitly in the boundary conditions. Also we used the two-term Galerkin approximation in the numerical computations. Dirichlet-type boundary conditions are used on the perturbation of temperature and concentration.

2. Mathematical formulation

The problem considered here is shown in figure 1. The Cartesian axes are chosen with the z^*-axis vertically upwards. The superscript asterisk denotes dimensional variables. The porous medium occupies a layer of height H. The vertical temperature difference and vertical concentration difference are ΔT and ΔC, respectively, across the boundaries. $(\beta_{T_x}, \beta_{T_y})$ and $(\beta_{C_x}, \beta_{C_y})$ are the imposed horizontal temperature and concentration gradient vectors, respectively. Under the Boussinesq approximation, the governing equations for the Darcy porous medium may be written in dimensional form as

$$\nabla^* \cdot \boldsymbol{v}^* = 0, \tag{1}$$

$$\boldsymbol{v}^* = \frac{K}{\mu}(-\nabla^* P^* + \rho_f^* g), \tag{2}$$

$$(\rho c)_m \left(\frac{\partial T^*}{\partial t^*}\right) + (\rho c_P)_f \boldsymbol{v}^* \cdot \nabla^* T^* = k_m \nabla^{*2} T^*, \tag{3}$$

$$\phi \left(\frac{\partial C^*}{\partial t^*}\right) + \boldsymbol{v}^* \cdot \nabla^* C^* = D_m \nabla^{*2} C^* + \frac{D_m k_m}{c_s c_p} \nabla^{*2} T, \tag{4}$$

where

$$\rho_f^* = \rho_0[1 - \gamma_T(T^* - T_0) - \gamma_C(C^* - C_0)].$$

The boundary conditions considered are of the form

$$\left.\begin{aligned} &w^* = 0,\ T^* = T_0 - \tfrac{1}{2}(\pm \Delta T) - \beta_{T_x} x^* - \beta_{T_y} y^*, \\ &C^* = C_0 - \tfrac{1}{2}(\pm \Delta C) - \beta_{C_x} x^* - \beta_{C_y} y^*,\ z^* = \pm \tfrac{1}{2} H. \end{aligned}\right\} \tag{5}$$

Here, $(u^*, v^*, w^*) = \boldsymbol{v}^*$is the Darcy velocity, $P^*$is the pressure, T^* and C^* are temperature and concentration, respectively. The subscripts m and f refer to the porous medium and the fluid, respectively. Also μ, ρ, c_s and c_p denote the viscosity, density, concentration susceptibility and specific heat at constant pressure, respectively. k_m and D_m denote the thermal and concentration diffusivities in the medium. Also γ_T and γ_C are the thermal and solutal expansion coefficients in the medium. Here, K and ϕ are the permeability and porosity of the medium. The coefficient $D_m k_m/(c_s c_p)$ which is added to the concentration equation is termed the Soret coefficient in the medium.

We introduce the following non-dimensional variables in the governing partial differential equations

$$x = \frac{x^*}{H}, \quad y = \frac{y^*}{H}, \quad z = \frac{z^*}{H}, \quad t = \frac{\alpha_m t^*}{AH^2}, \quad \boldsymbol{v} = \frac{H v^*}{\alpha_m}, \quad P = \frac{K(P^* + \rho_0 g z^*)}{\mu \alpha_m},$$

$$T = \frac{R_z(T^* - T_0)}{\Delta T}, \quad C = \frac{S_z(C^* - C_0)}{\Delta C},$$

where

$$\alpha_m = \frac{k_m}{(\rho c_p)_f}, \quad A = \frac{(\rho c)_m}{(\rho c_p)_f}, \quad R_z = \frac{\rho_0 g \gamma_T K H \Delta T}{\mu \alpha_m}, \quad S_z = \frac{\rho_0 g \gamma_C K H \Delta C}{\mu D_m}.$$

Here, R_z and S_z are the vertical thermal and solutal Rayleigh numbers, respectively. Also we introduce the horizontal thermal and solutal Rayleigh numbers as

$$R_x = \frac{\rho_0 g \gamma_T K H^2 \beta_{T_x}}{\mu \alpha_m}, \quad R_y = \frac{\rho_0 g \gamma_T K H^2 \beta_{T_y}}{\mu \alpha_m},$$

$$S_x = \frac{\rho_0 g \gamma_C K H^2 \beta_{C_x}}{\mu D_m}, \quad S_y = \frac{\rho_0 g \gamma_C K H^2 \beta_{C_y}}{\mu D_m}.$$

Under these non-dimensional variables, the governing equations (1)–(4) take the form

$$\nabla \cdot \boldsymbol{v} = 0, \tag{6}$$

$$v = -\nabla P + \left(T + \frac{1}{Le} C\right)\boldsymbol{k}, \tag{7}$$

$$\frac{\partial T}{\partial t} + \boldsymbol{v} \cdot \nabla T = \nabla^2 T, \tag{8}$$

$$(\phi/A)\frac{\partial C}{\partial t} + \boldsymbol{v} \cdot \nabla C = \frac{1}{Le} \nabla^2 C + S_r \nabla^2 T. \tag{9}$$

The transformed boundary conditions become

$$w = 0, \quad T = -\tfrac{1}{2}(\pm R_z) - R_x x - R_y y, \quad C = -\tfrac{1}{2}(\pm S_z) - S_x x - S_y y \text{ at } z = \pm\tfrac{1}{2}. \quad (10)$$

We recognize that the scaling used for time and velocity is somewhat arbitrary in a double-diffusive context. It has the advantage that it puts (3) and (4), in their simplest possible form and groups ϕ and A together in (9). This novel scaling of temperature and concentration has the effect of making R_z and S_z appear in the boundary conditions rather than in the differential equations. This has the consequence that all the Rayleigh numbers appear in the perturbation equations via the steady-state solutions only. The Lewis number Le is defined as the ratio of thermal and solutal diffusivities and is given by $Le = \alpha_m / D_m$. This shows that the solutal Rayleigh number can be expressed as $S_z = N Le R_z$ where N is the buoyancy ratio and is given by $\gamma_C \Delta C / (\gamma_T \Delta T)$. Here S_r is the Soret parameter and is given by $D_m k_m \Delta T S_z / (c_s c_p \alpha_m \Delta C R_z)$.

3. Steady-state solution

The governing equations admit a steady-state solution of the form

$$T_s = \tilde{T}(z) - R_x x - R_y y, \quad C_s = \tilde{C}(z) - S_x x - S_y y, \quad (11a)$$

$$u_s = U(z), \quad v_s = V(z), \quad w_s = 0, \quad P_s = P(x, y, z). \quad (11b)$$

with

$$\mathrm{D}U = R_x + \frac{S_x}{Le}, \quad \mathrm{D}V = R_y + \frac{S_y}{Le}, \quad (12a)$$

$$\mathrm{D}^2\tilde{T} = -U R_x - V R_y, \quad \frac{1}{Le}\mathrm{D}^2\tilde{C} = -U S_x - V S_y + S_r \mathrm{D}^2\tilde{T}. \quad (12b)$$

Here, D denotes the differentiation with respect to z.

When there is no net flow in the horizontal direction, we have $\langle U \rangle = 0, \quad \langle V \rangle = 0$, where $\langle\ \rangle$ represents integration with respect to z from $z = -\frac{1}{2}$ to $\frac{1}{2}$. Then we obtain the following solution for the flow, temperature and concentration in the medium

$$U = \left(R_x + \frac{S_x}{Le}\right) z, \quad V = \left(R_y + \frac{S_y}{Le}\right) z \quad (13a)$$

$$\tilde{T} = -R_z z + \tfrac{1}{24}\lambda_1 (z - 4z^3), \quad \tilde{C} = -S_z z + \tfrac{1}{24}\lambda_2 (z - 4z^3), \quad (13b)$$

where λ_1 and λ_2 are given by

$$\left.\begin{aligned} \lambda_1 &= R_x^2 + R_y^2 + \frac{R_x S_x + R_y S_y}{Le}, \\ \lambda_2 &= S_x^2 + S_y^2 + Le(R_x S_x + R_y S_y - S_r \lambda_1). \end{aligned}\right\} \quad (14)$$

Further, we define the thermal and solutal Rayleigh number vectors by $\boldsymbol{R} = (R_x, R_y, R_z)$ and $\boldsymbol{S} = (S_x, S_y, S_z)$. The flow given by (13) is the Hadley circulation and here it is in the vertical plane containing the vector $\boldsymbol{R} + \boldsymbol{S}/Le$.

4. Linear stability analysis

Consider the perturbations in the form $\boldsymbol{v} = \boldsymbol{v}_s + \boldsymbol{V}'$, $T = T_s + \theta'$, $C = C_s + c'$, $P = P_s + p'$, where the subscript s denotes steady-state solution and the prime represents the disturbance quantity. Upon substituting these perturbations into the non-dimensional

governing equations and neglecting the products of disturbances, the linearized perturbation equations are obtained as

$$\nabla \cdot \boldsymbol{V}' = 0, \tag{15}$$

$$\boldsymbol{V}' = -\nabla p' + \left(\theta' + \frac{1}{Le}c'\right)\boldsymbol{k}, \tag{16}$$

$$\frac{\partial \theta'}{\partial t} + U\frac{\partial \theta'}{\partial x} + V\frac{\partial \theta'}{\partial y} - R_x u' - R_y v' + (\mathrm{D}\tilde{T})w' = \nabla^2 \theta', \tag{17}$$

$$(\phi/A)\frac{\partial c'}{\partial t} + U\frac{\partial c'}{\partial x} + V\frac{\partial c'}{\partial y} - S_x u' - S_y v' + (\mathrm{D}\tilde{C})w' = \frac{1}{Le}\nabla^2 c' + S_r \nabla^2 \theta'. \tag{18}$$

Taking the normal modes of the form

$$[u', v', w', \theta', c', p'] = [u(z), v(z), w(z), \theta(z), c(z), p(z)] \exp\{\mathrm{i}(k x + l y - \sigma t)\} \tag{19}$$

and substituting in the above linearized perturbation equations (15)–(18) and further eliminating p, u and v from the resulting equations, we obtain

$$(\mathrm{D}^2 - \alpha^2)w + \alpha^2\left(\theta + \frac{1}{Le}c\right) = 0, \tag{20}$$

$$(\mathrm{D}^2 - \alpha^2 + \mathrm{i}\sigma - \mathrm{i}kU - \mathrm{i}lV)\theta + \mathrm{i}\frac{1}{\alpha^2}(kR_x + lR_y)\mathrm{D}w - (\mathrm{D}\tilde{T})w = 0, \tag{21}$$

$$\left(\frac{1}{Le}[\mathrm{D}^2 - \alpha^2] + \mathrm{i}(\phi/A)\sigma - \mathrm{i}kU - \mathrm{i}lV\right)c + \mathrm{i}\frac{1}{\alpha^2}(kS_x + lS_y)\mathrm{D}w - (\mathrm{D}\tilde{C})w + S_r(\mathrm{D}^2 - \alpha^2)\theta = 0, \tag{22}$$

where $\mathrm{D}\tilde{T} = -R_z + \lambda_1(1 - 12z^2)/24$ and $\mathrm{D}\tilde{C} = -S_z + \lambda_2(1 - 12z^2)/24$. The above eigenvalue system of equations (20)–(22) is solved subject to the boundary conditions

$$w = 0, \quad \theta = 0, \quad c = 0 \quad \text{at} \quad z = \pm\tfrac{1}{2}. \tag{23}$$

In the above, $\alpha = \sqrt{k^2 + l^2}$ is the overall wavenumber. The wavenumber vector is defined by $\boldsymbol{\alpha} = (k, l, 0)$. Now, refer to a disturbance with $\boldsymbol{\alpha}$ perpendicular to the direction of the Hadley circulation as a longitudinal mode and a disturbance with $\boldsymbol{\alpha}$ parallel to this plane as a transverse mode. For a longitudinal mode, the flow is composed of convective rolls, with axes aligned with the Hadley circulation, superposed upon that circulation. For a transverse mode, the roll axes are perpendicular to the Hadley circulation.

The above equations (20)–(23) constitute an eigenvalue problem for R_z with $Le, \phi, A, R_x, R_y, S_x, S_y, S_z, \sigma, k, l$ and S_r as parameters. The critical value of R_z is its minimum as σ, k and l are varied (with σ taking certain determined values).

5. Numerical procedure

The two-term Galerkin method is employed to find the eigenvalue R_z as suggested in Nield *et al.* (1993). The trial functions are chosen such that they satisfy the boundary conditions of the form

$$w_{2p-1} = \theta_{2p-1} = c_{2p-1} = \cos(2p-1)\pi z, \quad w_{2p} = \theta_{2p} = c_{2p} = \sin 2p\pi z \text{ for } p = 1, 2, \ldots$$

Now the second-order approximations for w, θ, c are in the following form:

$$w = \sum_{j=1}^{2} A_j w_j, \quad \theta = \sum_{j=1}^{2} B_j \theta_j, \quad c = \sum_{j=1}^{2} C_j c_j \tag{24}$$

We substitute these expressions into (20)–(22). Now we multiply the first of these equations by w_1, the second of these equations by θ_1 and the third of these equations by c_1. Similarly, repeat with w_2, θ_2 and c_2, then integrate each term with respect to z from $z = -1/2$ to $1/2$. After integrating by parts and using the boundary conditions, a system of six homogeneous linear equations in six unknowns A_1, A_2, B_1, B_2, C_1 and C_2 are obtained, this results in an eigenvalue problem in the form $\det(A_{m,n}) = 0$.

For $m, n = 1, 2$, the elements of the matrix are given by

$$\begin{aligned}
A_{3m-2,\,3n-2} &= \langle \mathrm{D}w_m\, \mathrm{D}w_n + \alpha^2 w_m\, w_n \rangle,\\
A_{3m-2,\,3n-1} &= -\alpha^2 \langle w_m\, \theta_n \rangle,\\
A_{3m-2,\,3n} &= -\alpha^2 \frac{1}{Le} \langle w_m\, c_n \rangle,\\
A_{3m-1,\,3n-2} &= \left\langle \mathrm{D}\tilde{T}\, \theta_m w_n - \mathrm{i}\frac{1}{\alpha^2}(kR_x + lR_y)\theta_m\, \mathrm{D}w_n \right\rangle,\\
A_{3m-1,\,3n-1} &= \left\langle \mathrm{D}\theta_m\, \mathrm{D}\theta_n + (\alpha^2 - \mathrm{i}[\sigma - kU - lV])\theta_m\, \theta_n \right\rangle,\\
A_{3m-1,\,3n} &= 0,\\
A_{3m,\,3n-2} &= \left\langle \mathrm{D}\tilde{C}\, c_m\, w_n - \mathrm{i}\frac{1}{\alpha^2}(kS_x + lS_y)c_m\, \mathrm{D}w_n \right\rangle,\\
A_{3m,\,3n-1} &= \langle S_r\, (\mathrm{D}c_m\, \mathrm{D}\theta_n + \alpha^2 c_m\, \theta_n) \rangle,\\
A_{3m,\,3n} &= \left\langle \frac{1}{Le}\mathrm{D}c_m\, \mathrm{D}c_n + (\alpha^2 - \mathrm{i}[(\phi/A)\sigma - kU - lV])c_m\, c_n \right\rangle.
\end{aligned}$$

The various integrals involved in the above can easily be evaluated. For example,

$$\begin{aligned}
\langle w_m \quad w_n \rangle &= \tfrac{1}{2}\delta_{m\,n}, \quad \langle \mathrm{D}w_m \quad \mathrm{D}w_n \rangle = \tfrac{1}{2}m^2\pi^2\,\delta_{mn},\\
\langle z\,\theta_m \quad w_n \rangle &= \frac{4mn\,\nu_{mn}}{\pi^2(m^2 - n^2)^2},\\
\langle z^2\,\theta_m \quad w_n \rangle &= \left(\frac{1}{24} - \frac{1}{4\pi^2 n^2}\right)\delta_{mn},\\
\langle \theta_m \quad \mathrm{D}w_n \rangle &= \frac{2mn\,\nu_{m\,n}}{n^2 - m^2},
\end{aligned}$$

$$\text{where } \nu_{m\,n} = \begin{cases} 0 & \text{if } m+n \text{ is even,}\\ 1 & \text{if } \tfrac{1}{2}(m+n+1) \text{ is even,}\\ -1 & \text{if } \tfrac{1}{2}(m+n+1) \text{ is odd,} \end{cases}$$

Hence, we find the elements of the matrix $\boldsymbol{A}$ as

$$\begin{aligned}
&A_{11} = \tfrac{1}{2}(\pi^2 + \alpha^2),\ A_{12} = -\tfrac{1}{2}\alpha^2,\ A_{13} = -\frac{1}{2\,Le}\alpha^2,\ A_{14} = A_{15} = A_{16} = 0,\\
&A_{21} = -\tfrac{1}{2}R_z + \frac{\lambda_1}{8\pi^2},\ A_{22} = \tfrac{1}{2}(\pi^2 + \alpha^2 - \mathrm{i}\sigma),\ A_{23} = 0,
\end{aligned}$$

$$A_{24} = -4\mathrm{i}\frac{\alpha\cdot\boldsymbol{R}}{3\alpha^2},\ A_{25} = -8\mathrm{i}\frac{\left\{\alpha\cdot\boldsymbol{R} + \frac{1}{Le}\alpha\cdot\boldsymbol{S}\right\}}{9\pi^2},\ A_{26} = 0,$$

$$A_{31} = -\tfrac{1}{2}s_z + \frac{\lambda_2}{8\pi^2},\ A_{32} = \frac{S_r}{2}(\pi^2+\alpha^2),\ A_{33} =,\ \tfrac{1}{2}\left\{\frac{1}{Le}(\pi^2+\alpha^2) - \mathrm{i}(\phi/A)\sigma\right\},$$

$$A_{34} = -4\mathrm{i}\frac{\alpha\cdot\boldsymbol{S}}{3\alpha^2},\ A_{35} = 0,\ A_{36} = 8\mathrm{i}\frac{\left\{\alpha\cdot\boldsymbol{R} + \frac{1}{Le}\alpha\cdot\boldsymbol{S}\right\}}{9\pi^2},$$

$$A_{41} = A_{42} = A_{43} = 0,\ A_{44} = \tfrac{1}{2}(\pi^2+\alpha^2),\ A_{45} = -\tfrac{1}{2}\alpha^2,\ A_{46} = -\tfrac{1}{2\,Le}\alpha^2,$$

$$A_{51} = 4\mathrm{i}\frac{\alpha\cdot\boldsymbol{R}}{3\alpha^2},\ A_{52} = 8\mathrm{i}\frac{\left\{\alpha\cdot\boldsymbol{R} + \frac{1}{Le}\alpha\cdot\boldsymbol{S}\right\}}{9\pi^2},\ A_{53} = 0,$$

$$A_{54} = -\tfrac{1}{2}R_z + \frac{\lambda_1}{32\pi^2},\ A_{55} = \tfrac{1}{2}(4\pi^2+\alpha^2 - i\sigma),\ A_{56} = 0,$$

$$A_{61} = 4i\,\frac{\alpha\cdot\boldsymbol{S}}{3\alpha^2},\ A_{62} = 0,\ A_{63} = 8\mathrm{i}\frac{\left\{\alpha\cdot\boldsymbol{R} + \frac{1}{Le}\alpha\cdot\boldsymbol{S}\right\}}{9\pi^2}$$

$$A_{64} = -\tfrac{1}{2}s_z + \frac{\lambda_2}{32\pi^2},\ A_{65} = \frac{S_r}{2}(4\pi^2+\alpha^2),\ A_{66} =,\ \tfrac{1}{2}\left\{\frac{1}{Le}(4\pi^2+\alpha^2) - \mathrm{i}(\phi/A)\sigma\right\}.$$

Since the matrix is of order 6×6, and involves large parameter space, it is difficult to find a dispersion relation between the critical vertical Rayleigh number R_z and the wavenumber α; but this can be obtained in one special case. If $\boldsymbol{R}$ and $\boldsymbol{S}$ lie in the same vertical plane, then for the longitudinal modes we have $\alpha\cdot\boldsymbol{R} = \boldsymbol{\alpha}\cdot\boldsymbol{S} = \boldsymbol{0}$, the sixth-order determinant factorizes into the product of two third-order determinants and the eigenvalue equation splits into two equations. One of these corresponds to an even mode and the other corresponds to an odd mode. These modes can then be dealt with separately. The real and imaginary parts of the eigenvalue equation yield two equations, involving real quantities, to be solved simultaneously. Now there are two alternatives for finding these dispersion relations:

$$\sigma = 0,\ R_z + S_z - S_r\,R_z - \frac{(\lambda_1+\lambda_2 - S_r\,\lambda_1)}{4\pi^2} = \frac{(\pi^2+\alpha^2)}{\alpha^2} \tag{25}$$

or

$$\left(\frac{\phi\,Le}{A}\right)\sigma^2 = (\pi^2+\alpha^2)^2 - \alpha^2\left[R_z + S_z - S_r\,R_z - \frac{(\lambda_1+\lambda_2 - S_r\,\lambda_1)}{4\pi^2}\right], \tag{26}$$

$$\left(\frac{\phi\,Le}{A}\right)\left(R_z - \frac{\lambda_1}{4\pi^2}\right) + \left(S_z - \frac{\lambda_2}{4\pi^2}\right) = \left[1 + \frac{\phi\,Le}{A}\right]\ \frac{(\pi^2+\alpha^2)}{\alpha^2}. \tag{27}$$

As α varies, the minimum value of $(\pi^2+\alpha^2)/\alpha^2$ is $4\pi^2$ and it is attained at $\alpha = \pi$. From this, it is found that for the neutral stability curve for the non-oscillatory modes, the dispersion relation for critical Rayleigh number is given by

$$R_z + S_z - S_r\,R_z = 4\pi^2 + \frac{(\lambda_1+\lambda_2 - S_r\,\lambda_1)}{4\pi^2} \tag{28}$$

and for the oscillatory modes it is given by

$$\left(\frac{\phi\, Le}{A}\right)\left(R_z - \frac{\lambda_1}{4\pi^2}\right) + \left(S_z - \frac{\lambda_2}{4\pi^2}\right) = 4\pi^2\left[1 + \frac{\phi\, Le}{A}\right], \tag{29}$$

which are same as those given in Nield *et al.* (1993) for the horizontal gradient case in the absence of Soret effect. The second factor corresponds to the second lowest eigenvalue and yields the same relation at $\alpha = \pi$ with the minimum value $16\pi^2$. The above relations provide only upper bounds on the critical vertical Rayleigh number, for the coplanar case.

6. Results and discussion

For the most general case, the equation $\det(A_{m,n}) = 0$ is solved to obtain the critical vertical Rayleigh number. Usage of polar coordinates for the horizontal vectors facilitates the procedure and the transformation given in Nield *et al.* (1993) is used here also with an exception that in the present case, both $\psi_S$and ψ_R are given non-zero values.

$$k = \alpha \cos\psi, \quad l = \alpha \sin\psi,$$
$$R_x = R_H \cos\psi_R, \quad R_y = R_H \sin\psi_R,$$
$$S_x = S_H \cos\psi_S, \quad S_y = S_H \sin\psi_S.$$

The real and imaginary parts of the determinant gives two equations, one corresponds to the real part, i.e. $\mathrm{Re}(R_z)$, and the other corresponds to the imaginary part, $\mathrm{Im}(R_z)$, both are quadratic in R_z. These two equations are to be solved simultaneously for R_z. Here, the $\mathrm{Im}(R_z) = 0$ is a fourth-degree polynomial equation in σ, solving which we find the values of σ in terms of other parameters. Using these values of σ, the values of R_z are found from $\mathrm{Re}(R_z) = 0$. For each value of σ, the parameters α and ψ are varied to obtain the minimum value of $\mathrm{Re}(R_z)$. The smallest of these values of R_z is its critical value. We used *Mathematica* for the above calculations. In the present study, we used a fixed value for the ratio φ/A as equal to 1. Extensive calculations have been made for the following range of parameters, $-50 \leqslant S_z \leqslant 100$, $0 \leqslant R_H \leqslant 100$, $-50 \leqslant S_H \leqslant 100$, $-1 \leqslant S_r \leqslant 1$, $0^\circ \leqslant \psi \leqslant 180^\circ$ and $0^\circ \leqslant \psi_R,\ \psi_S \leqslant 180^\circ$ with the Lewis number varying in the range $0.05 \leqslant Le \leqslant 500$. For $\psi_R = 0$, i.e. when the thermal and solutal gradients are coplanar, there is further symmetry which allowed a restriction on the interval $0^\circ \leqslant \psi \leqslant 90^\circ$.

Variation of critical R_z is tabulated for different values of the Soret parameter and vertical solutal Rayleigh number S_z in the absence of the horizontal thermal and solutal Rayleigh numbers (table 1*a*) and in the presence of the horizontal thermal and solutal Rayleigh numbers (table 1*b*). The present results are compared with the existing results in the literature with the available data in the chosen parameter space. From table 1, it is clearly seen that when S_r is zero, the present results with two-term Galerkin approximation are in very good agreement with the existing results in the literature (Guo & Kaloni 1995). The critical values of the wavenumbers are observed to match with the values presented in their work. Also, it is seen that an increase in the vertical solutal Rayleigh number reduced the critical value of R_z and it shows that the Soret parameter has a stabilizing effect in the medium.

The effect of the diffusivity ratio parameter on the critical value of R_z is shown for varying Soret parameter values for both the positive (table 2*a*) and negative (table 2*b*) values of S_z. From the comparison made in table 2(*a*), it is evident that the present

	S_z	−30	−20	−10	0	10	20	30
(*a*)	$S_r = 0$ (present)	69.5102	59.5102	49.5102	39.5102	29.5102	19.5102	9.51024
	Guo & Kaloni (1995)	69.48	59.48	49.48	39.48	29.48	19.48	9.48
	$S_r = 0.1$	77.2336	66.1225	55.0114	43.9003	32.7892	21.678	10.5669
	$S_r = -0.1$	63.1911	54.510	45.0095	35.9184	26.8275	17.7366	8.64567
(*b*)	$S_r = 0$ (present)	69.7383	59.7663	49.798	39.8336	29.8729	19.9161	9.96307
	Guo & Kaloni (1995)	70.09	60.09	50.09	40.09	30.09	20.09	10.09
	$S_r = 0.1$	77.4275	66.348	55.2737	44.2046	33.1408	22.6822	11.0288
	$S_r = -0.1$	63.445	66.348	55.2737	44.2046	33.1408	22.6822	11.0288

TABLE 1. Critical thermal Rayleigh numbers for (*a*) $R_H = S_H = 0$ and (*b*) $R_H = S_H = 1$ with $\sigma = 0$.

	Le	0.05	0.5	1	10	50	250	500
(*a*)	$S_r = 0$ (present)	29.4319	29.5882	29.5894	29.8729	31.6516	38.6286	39.989
	Guo & Kaloni (1995)	30.60	29.71	29.68	30.09	32.11	42.25	54.91
	$S_r = 0.1$	32.6525	32.863	32.8649	33.1408	34.7021	39.6441	40.2882
	$S_r = -0.1$	26.8011	26.9053	26.9057	27.197	29.1307	37.6987	39.7246
(*b*)	$S_r = 0$	48.9841	49.5735	49.5806	49.798	50.1121	45.278	42.2788
	$S_r = 0.1$	54.3751	55.0709	55.0794	55.2737	55.0981	46.6887	42.639
	$S_r = -0.1$	44.5728	45.0754	45.0814	45.3152	45.988	43.997	41.9375

TABLE 2. Critical thermal Rayleigh numbers for $R_H = S_H = 1$ and (*a*) $S_z = 10$ and (*b*) $S_z = -10$ with $\sigma = 0$.

results with the two-term Galerkin approximation are in excellent agreement with the results obtained using the compound matrix method in Guo & Kaloni (1995). From table 2(*a*), it is observed that for $S_z > 0$, increasing the value of *Le* increased the value of R_z. Whereas for $S_z < 0$ (table 2*b*), it is clear that as *Le* increased, the critical value of R_z increases up to a certain value and thereafter reduces.

A fixed notation is used to represent the curves corresponding to the non-oscillatory and oscillatory modes. Solid lines represent non-oscillatory modes whereas the dashed lines represent oscillatory modes in figures 2 to 7.

In figure 2, the response of the critical vertical thermal Rayleigh number R_z against S_z is shown for the case of $R_H = S_H = 0$ and $\psi = 0$. The effect of the Soret parameter on both oscillatory and non-oscillatory modes is also shown. It is evident from this figure that the oscillatory modes are much more stable than the non-oscillatory modes. Also it is observed that increasing S_z in the medium has a destabilizing effect on non-oscillatory modes. Note that in the case of inclined thermal and solutal gradients, an increase in the value of the Soret parameter stabilizes the non-oscillatory modes up to a certain value of S_z, beyond which it starts destabilizing these modes. For the oscillatory modes, it is observed that an increase in vertical solutal Rayleigh number has a stabilizing effect whereas increase in S_r destabilized these oscillatory modes marginally. These graphs are plotted for $S_r = 0, 0.1, 0.5$.

In figure 3, variation of R_z is shown as a function of S_z for varying $S_r = 0, 0.1$ for the case of non-zero horizontal solutal gradient, $S_H = 20$. In this case also, an increase in vertical solutal Rayleigh number destabilized both these modes, whereas

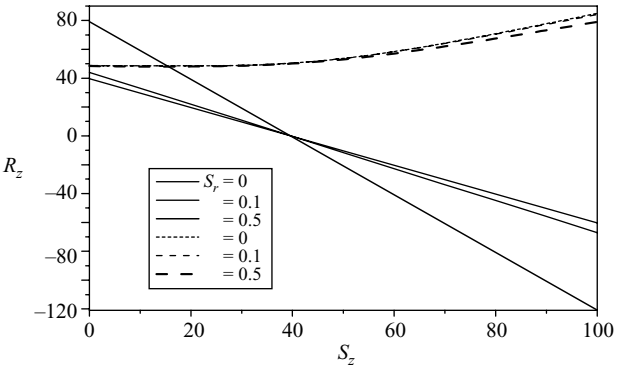

FIGURE 2. Variation of critical value of R_z against S_z for varying S_r with $R_H = S_H = 0$.

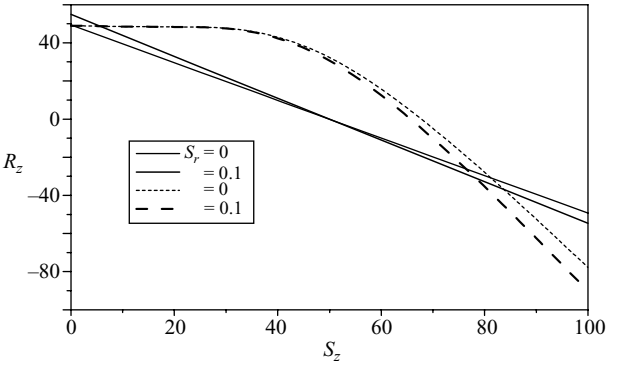

FIGURE 3. Variation of critical value of R_z against S_z for varying $S_r = 0, 0.1$ with $R_H = 0$, $S_H = 20$.

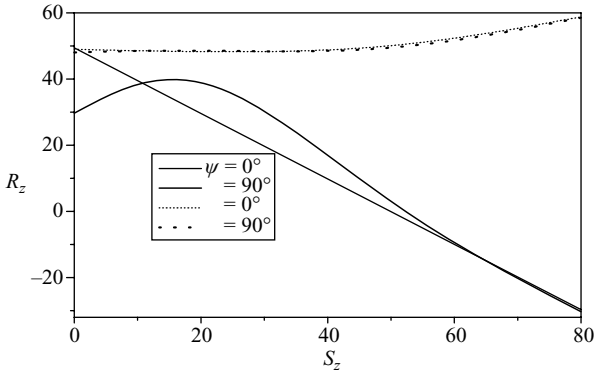

FIGURE 4. Variation of critical value of R_z against S_z for fixed $S_r = 0$ with $\psi = 0°,\ 90°$ for $R_H = S_H = 0, 20$ with varying $\psi_R,\ \psi_s$.

an increase in S_r showed a similar effect after some critical value of S_z. With non-zero values for S_H, it is observed that the oscillatory modes switch over to non-oscillatory modes as S_z increases further.

The critical value of R_z is plotted against S_z for $\psi = 0°$ and $\psi = 90°$ with $R_H = S_H = 20$ and varying $\psi_S,\ \psi_R$ in the absence of the Soret effect in the medium in figure 4. It

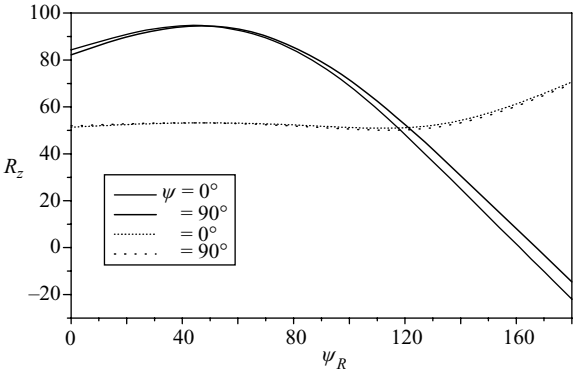

FIGURE 5. Variation of critical value of R_z against ψ_S for fixed $S_r = 0.1$, $S_z = 10$, $R_H = S_H = 20$ for $\psi = 0°, 90°$.

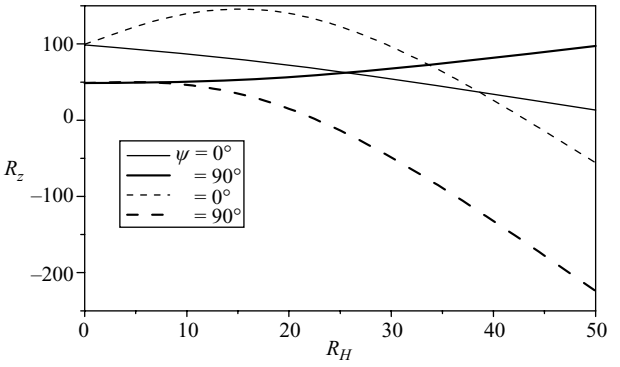

FIGURE 6. Variation of critical value of R_z against R_H with fixed $S_r = 0.5$, $S_z = 0$ and $S_H = 20$ with $\psi = 0°, 90°$.

is observed that the non-oscillatory modes are becoming unstable while the oscillatory modes are stabilized with increasing S_z. An increase in ψ reduced the critical value of R_z with increasing value of S_z. However, for the non-oscillatory modes, a distinct phenomenon is observed. Increasing the value of ψ reduced the critical value of R_z up to certain value of S_z; beyond this value of S_z, the critical value of R_z increases.

Variation of R_z against ψ_R is shown in figure 5 for two values of $\psi = 0°$ and $\psi = 90°$. These graphs are plotted for fixed $\psi_S = 45°$, $S_z = 10$, $R_H = S_H = 20$ and $S_r = 0.1$. From this figure, it is clear that the non-oscillatory modes are much more stable than oscillatory modes up to a certain value of ψ_R and become destabilized for all values beyond this value of ψ_R. The oscillatory modes are stabilized with increasing value of ψ_R.

From figure 6 where R_z is plotted as a function of R_H for $\psi = 0°$ and $\psi = 90°$ when $S_r = 0.5$, it is evident that the critical R_z for non-oscillatory modes is decreasing for $\psi = 0°$ whereas it is increasing for $\psi = 90°$ with increasing value of R_H. However, for oscillatory modes, the critical value of R_z is decreasing with increasing values of ψ. When $\psi = 0°$, the horizontal thermal Rayleigh number shows a dual effect on R_z.

The aim of the present analysis is to show the influence of the Soret parameter on the critical vertical thermal Rayleigh number R_z of both the oscillatory and non-oscillatory modes. This is shown in figure 7 for two values of ψ with fixed $R_H = S_H = 0$ and $S_z = 0$. From this, it is clear that the non-oscillatory modes are

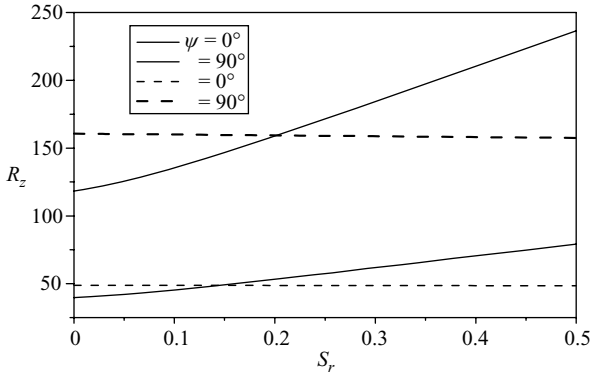

FIGURE 7. Variation of critical value of R_z against S_r with $R_H = S_H = 0$, keeping other parameters constant for $\psi = 0°, 90°$.

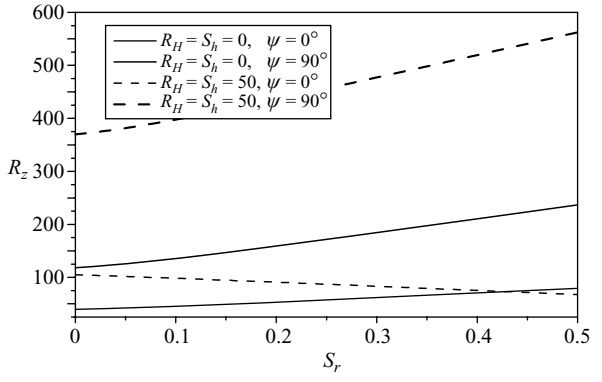

FIGURE 8. Variation of critical value of R_z against S_r with $R_H = S_H = 0$, 50 with $\psi = 0°$, 90°, keeping other parameters fixed for $\psi = 0°, 90°$.

stable with increasing value of S_r and the critical value of R_z is observed to increase with increasing values of ψ. However, for the oscillatory modes, the critical value of R_z is decreasing slightly as S_r increases and, as the value of ψ increases, the critical value of R_z increases for these modes also.

The variation of critical R_z against the Soret parameter S_r is plotted in figure 8, for the stationary modes with $R_H = S_H = 0$ and 50; and $\psi = 0°$ and 90°. Solid lines represent $R_H = S_H = 0$ and dashed lines represent $R_H = S_H = 50$. For the former case, stationary modes are stabilized with increasing value of ψ as S_r increases. The critical value of R_z is increased with the Soret parameter S_r. However, because of the presence of horizontal gradients (in the latter case), the critical value of R_z is reduced with increasing S_r for $\psi = 0°$ and the Soret parameter showed a stabilizing effect when $\psi = 90°$.

In figure 9, the difference between critical values of R_z for non-oscillatory and oscillatory modes with varying S_r is plotted for $R_H = S_H = 0$ (case 1), 50 (case 2) and 100 (case 3), with $\psi = 0°$ and $\psi = 90°$. Solid lines represent plots for $\psi = 0°$ and dashed lines represents for $\psi = 90°$. Case 1 indicates that there are no horizontal thermal and solutal gradients, for which there is no significant difference in the critical vertical thermal Rayleigh number R_z and it is clear from this figure that the Soret parameter has no significant effect on R_z compared with case 3 where horizontal

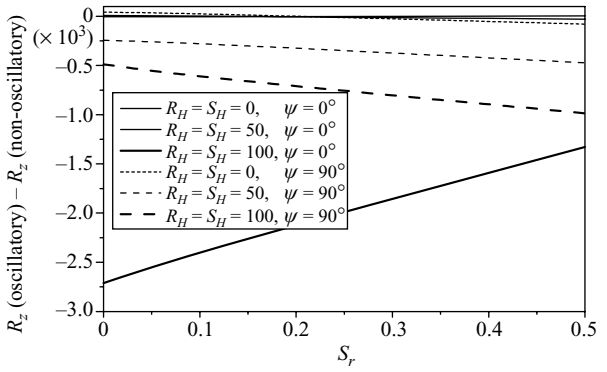

FIGURE 9. Difference between the oscillatory and non-oscillatory modes of R_z against S_r with $R_H = S_H = 0,\ 50,\ 100$, keeping other parameters constant for $\psi = 0°, 90°$.

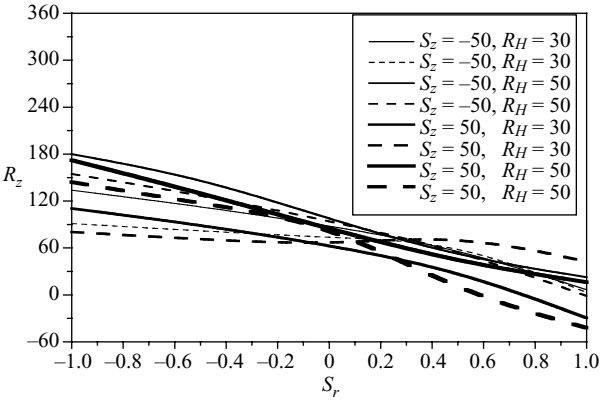

FIGURE 10. Variation of R_z against S_r for varying S_z and R_H with fixed $Le = 10$, and $S_H = 10$ for $\psi = \psi_R = \psi_S = 0$. Solid lines are non-oscillatory and dashed lines are oscillatory modes.

thermal and solutal gradients are present. In this case, it is seen that the difference in the critical values of R_z considered is decreasing for $\psi = 0°$ whereas the same is increasing rapidly for $\psi = 90°$ as the value of the Soret parameter Sr increases.

In figure 10, variation of the vertical thermal Rayleigh number R_z, is shown against positive and negative values of the Soret parameter for both negative and positive values of S_z. Two possibilities can arise for S_z: (i) when the concentration on the upper plane is greater than that on the lower plane, the sign of S_z is positive; (ii) when the concentration on the lower plane is greater than that on the upper plane, the sign of S_z is negative. For the negative value of S_z, an increase in the horizontal thermal Rayleigh number shows a stabilizing effect on non-oscillatory modes up to some critical values of the Soret parameter. Beyond this value of the Soret parameter, these modes are observed to be destabilized. For positive values of S_z, increasing the value of the horizontal thermal Rayleigh number showed a destabilizing effect on non-oscillatory modes. From all these observations, it is evident that an increase in the Soret parameter value reduced the critical value of the vertical thermal Rayleigh number in the medium.

For oscillatory modes, it is observed that the horizontal thermal Rayleigh number exhibits a dual role on the critical vertical thermal Rayleigh number in the medium

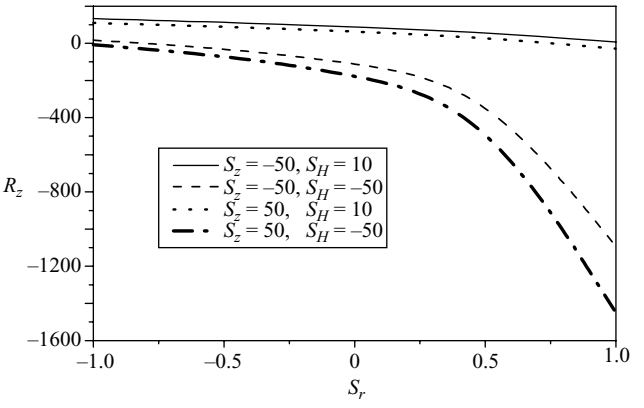

FIGURE 11. Variation of critical R_z for non-oscillatory modes with S_r with varying vertical and horizontal solutal Rayleigh numbers for $R_H = 30$, $Le = 10$ for $\psi = \psi_R = \psi_S = 0$.

for negative and positive values of S_z. When $R_H = 50$, the value of R_z is more than that for $R_H = 30$ up to certain values of the Soret parameter. Beyond this critical value of Sr, for $R_H = 50$, the value of R_z is less than that for $R_H = 30$. Also, the Soret parameter shows a dual role on oscillatory modes for $R_H = 30$.

In figure 11, variation of critical R_z is shown against the Soret parameter for non-oscillatory modes with varying solutal Rayleigh numbers in the medium. It is observed that these modes are destabilized with increasing values of the Soret parameter. When S_z is negative, the critical value of R_z is more than in the other case. When the horizontal solutal Rayleigh S_H number is negative, the critical value of R_z is comparatively less than in the other case. When $S_H > 0$, the critical value of R_z decreases linearly whereas a nonlinear reduction for R_z is observed for negative horizontal solutal Rayleigh numbers against the Soret parameter S_r.

In figure 12, variation of critical R_z is shown as a function of the Soret parameter in the absence and presence of the horizontal thermal and solutal Rayleigh numbers in the medium for non-oscillatory modes (figure 12*a*) and for oscillatory modes (figure 12*b*). From (figure 12*a*), it can be seen that when $S_z < 0$, the Soret parameter shows a stabilizing effect in the absence of horizontal thermal and solutal Rayleigh numbers whereas in the presence of these horizontal Rayleigh numbers, these modes are destabilized. When the vertical solutal Rayleigh number is positive, i.e. $S_z > 0$, an increase in the Soret parameter value showed a destabilizing effect in the absence and presence of the horizontal gradients in the medium. From (figure 12*b*), it can be seen that as the value of the Soret parameter is increased, the critical value of R_z is increasing in the absence of horizontal gradients. Also, it is observed that the critical value of R_z is more for $S_z < 0$ than in the other case. However, a distinct feature is seen in the presence of these horizontal Rayleigh numbers. For $S_z < 0$, the critical value of R_z is more than that of the other case up to certain value of the Soret parameter. Beyond this value of S_r, when $S_z < 0$, the critical value of R_z is less than the value of R_z when $S_z > 0$, and decreases with S_r.

In order to analyse the effect of Le on the critical value of R_z, we have shown the variation of R_z against the Soret parameter with three different value of Le for non-oscillatory modes in figure 13. When $Le \leqslant 1$, an increase in the Soret parameter shows the stabilizing effect for negative values of S_z, whereas these modes are destabilized for

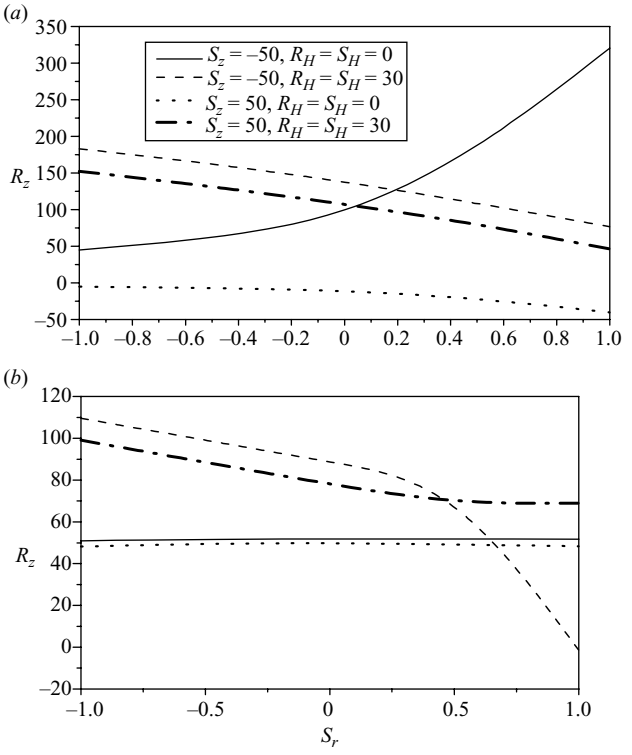

FIGURE 12. Variation of critical value of R_z against the Soret parameter S_r, for negative and positive values of S_z in the absence and presence of horizontal thermal and solutal Rayleigh numbers (*a*) non-oscillatory modes and (*b*) oscillatory modes for $\psi = \psi_R = \psi_S = 0$. $Le = 10$.

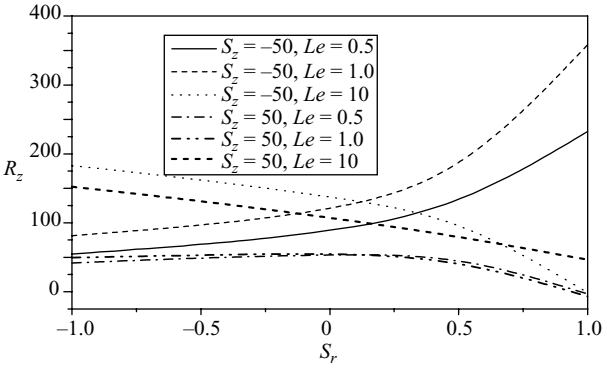

FIGURE 13. Critical values of R_z for non-oscillatory modes against the Soret parameter S_r for three different values of the diffusivity ratio parameter Le for $\psi = \psi_R = \psi_S = 0$. $R_H = S_H = 30$.

$Le > 1$. However, for positive values of S_z, an increase in the Soret parameter reduced the critical value of R_z, whereas the value of R_z is increased with the diffusivity ratio parameter.

7. Conclusion

The effect of the Soret parameter on the thermosolutal convection induced by inclined thermal and solutal gradients in a horizontal layer of a porous medium is studied using a linear stability analysis. The horizontal components of these gradients induce a Hadley circulation, which becomes unstable when the vertical component of the Solutal Rayleigh number is large. Usual three-dimensional normal modes are assumed for the disturbances and the resultant eigenvalue problem has been solved using a two-term Galerkin method. The present results for the zero Soret parameter case are compared with the existing results in the published literature which were obtained using a compound matrix method, and the comparison shows very good agreement. The vertical component of the thermal Rayleigh number has been treated as the eigenvalue of the system and variation of this parameter is shown as a function of the governing parameters of the flow. When the thermal and solutal Rayleigh numbers lie on the same plane, a dispersion relation is achieved for the vertical thermal Rayleigh number as a function of the overall wavenumber with Soret effect in the medium. The effect of the Soret parameter on the critical value of the vertical thermal Rayleigh number is observed in the absence and presence of the horizontal gradients. It is observed that in the absence of horizontal gradients, the Soret parameter plays a dual role on non-oscillatory modes with respect to the vertical solutal Rayleigh number in the medium while the Soret parameter always showed a destabilizing effect on these modes. A similar observation is made when the horizontal thermal gradients are absent and horizontal solutal gradients are present. In the absence of horizontal thermal and solutal Rayleigh numbers, it is observed that critical values of the vertical thermal Rayleigh number are reduced with the vertical solutal Rayleigh number whereas this critical value is increased with the Soret parameter. Similar behaviour is observed with the Soret parameter and vertical solutal gradients when both the horizontal gradients are present. When the vertical solutal Rayleigh number is positive, the critical value of the vertical thermal Rayleigh number increased with the increasing diffusivity ratio parameter while a dual role with respect to this diffusivity ratio parameter is seen for negative values of the vertical solutal Rayleigh number.

The authors are grateful to the reviewers for their constructive criticism which helped us to improve this paper. Also, P. A. L. N. and P. V. S. N. M. would like to acknowledge sincerely the financial assistance received from the CSIR, India through the research project grant number 25(155)/07/EMR-II.

REFERENCES

Alex, M. S. & Patil, P. R. 2001 Effect of variable gravity field on Soret driven thermosolutal convection in a porous medium. *Intl Commun. Heat Mass Transfer* **28**, 509–518.

Alex, S. M. & Patil, P. R. 2002 Effect of a variable gravity field on thermal instability in a porous medium with inclined temperature gradient and vertical through flow. *J. Porous Media* **5**, 137–147.

Alex, S. M., Patil, P. R. & Venkatakrishnan, K. S. 2001 Variable gravity effects on thermal instability in a porous medium with internal heat source and inclined temperature gradient. *Fluid. Dyn. Res.* **29**, 1–6.

Bahloul, A., Boutana, N. & Vasseur, P. 2003 Double-diffusive and Soret-induced convection in a shallow horizontal porous layer. *J. Fluid Mech.* **491**, 325–352.

Bhattacharyya, S. P. & Nadoor, S. 1976 Stability of thermal convection between non-uniformly heated plates. *Appl. Sci. Res.* **32**, 555–570.

Caldwell, D. R. 1976 Thermosolutal convection in a solution with large negative Soret coefficient. *J. Fluid Mech.* **74**, 129–142.

Costesèque, P., Fargue, D. & Jamet, Ph. 2002 Thermodiffusion in porous media and its consequences. In *Thermal Nonequilibrium Phenomena in Fluid Mixtures*. Lecture Notes in Physics, vol. 584, pp. 389–427. Springer.

Delahaye, R., Bahloul, A. & Vasseur, P. 2002 Influence of the Soret effect on convection in a binary fluid layer with a free upper surface. *Intl Commun. Heat Mass Transfer* **29**, 433–442.

Eckert, E. R. G. & Drake, R. M. 1972 *Analysis of Heat and Mass Transfer*. McGraw-Hill.

Hurle, D. T. J. & Jakeman, E. 1971 Soret-driven thermosolutal convection. *J. Fluid Mech.* **47**, 667–687.

Guo, J. & Kaloni, P. N. 1995 Nonlinear stability and convection induced by inclined thermal and solutal gradients. *Z. Angew. Math. Phys.* **46**, 645–654.

Kaloni, P. N. & Qiao, Z. 1997 Non-linear stability of convection in a porous medium with inclined temperature gradient. *Intl J. Heat Mass Transfer* **40**, 1611–1615.

Kaloni, P. N. & Qiao, Z. 2001 Nonlinear convection in a porous medium with inclined temperature gradient and variable gravity effects. *Intl J. Heat Mass Transfer* **44**, 1585–1591.

Lage, J. L. & Nield, D. A. 1998 Convection induced by inclined gradients in a shallow porous medium layer. *J. Porous Media*, **1**, 57–69.

Manole, D. M. & Lage, J. L. 1995 Numerical simulation of supercritical Hadley circulation, within a porous layer, induced by inclined temperature gradients. *Intl J. Heat Mass Transfer* **38**, 25-83-2593.

Manole, D. M., Lage, J. L. & Nield, D. A. 1994 Convection induced by inclined thermal and solutal gradients, with horizontal mass flow, in a shallow horizontal layer of a porous medium. *Intl J. Heat Mass Transfer* **37**, 2047–2057.

Manole, D. M., Lage, J. L. & Antohe, B. V. 1995 Supercritical Hadley circulation within a layer of fluid saturated porous medium: bifurcation to traveling wave. *ASME HTD* **309**, 23–29.

Mortimer, G. R. & Eyring, H. 1980 Elementary transition state theory of the Soret and Dufour effects. *Proc. Natl Acad. Sci. USA, Chem.* **77**, 1728–1731.

Nield, D. A. 1990 Convection in a porous medium with inclined temperature gradient and horizontal mass flow. *Heat Transfer 1990*, vol. 5, pp. 153–158. Hemisphere.

Nield, D. A. 1991 Convection in a porous medium with inclined temperature gradient. *Intl J. Heat Mass Transfer* **34**, 87–92.

Nield, D. A. 1994 Convection in a porous medium with inclined temperature gradient: additional results. *Intl J. Heat Mass Transfer* **37**, 3021–3025.

Nield, D. A. 1998 Convection in a porous medium with inclined temperature gradient and vertical through flow. *Intl J. Heat Mass Transfer* **41**, 241–243.

Nield, D. A. & Bejan, A. 2006 *Convection in Porous Media*, 3rd Edn. Springer.

Nield, D. A., Manole, D. M. & Lage, J. L. 1993 Convection induced by inclined thermal and solutal gradients in a shallow horizontal layer of a porous medium. *J. Fluid Mech.* **257**, 559–574.

Ouriemi, M., Vasseur, P. & Bahloul, A. 2005 Natural convection of a binary mixture confined in a slightly inclined tall enclosure. *Intl Commun. Heat Mass Transfer*. **32**, 770–778.

Parthiban, C. & Patil, P. R. 1993 Effect of inclined temperature gradient on thermal instability in an anisotropic porous medium. Wärme-Stoffübertrag. **29**, 63–69.

Parthiban, C. & Patil, P. R. 1994 Effect of inclined gradients on thermohaline convection in porous medium. Wärme-Stoffübertrag. **29**, 291–297.

Parthiban, C. & Patil, P. R. 1997 Thermal instability in an anisotropic porous medium with internal heat source and inclined temperature. *Intl Commun. Heat Mass Transfer* **24**, 1049–1058.

Platten, J. K. 2006 The Soret effect: a review of recent experimental results. *Trans. ASMEE: J. Appl. Mech.* **73**, 5–15.

Platten, J. K. & Chavepeyer, G. 1973 Oscillatory motion in Bénard cell due to the Soret effect. *J. Fluid Mech.* **60**, 305–319.

Platten, J. K., Dutrieux, J. F. & Chavepeyer, G. 2002 Soret effect and free convection: a way to measure Soret coefficients. In *Thermal Nonequilibrium Phenomena in Fluid Mixtures*. Lecture Notes in Physics, vol. 584, pp. 313–333. Springer.

Platten, J. K., Bou-Ali, M. M., Costeseque, P., Kohler, W., Leppla, C., Wiegand, S. & Wittko, G. 2003 Benchmark values for the Soret effect, thermaldiffusion and diffusion coefficients of three binary organic liquid mixtures. *Phil. Mag.* **83**, 1965–1971.

Qiao, Z. & Kaloni, P. N. 1997 Convection induced by inclined temperature gradient with mass flow in a porous medium. *Trans. ASME J. Heat Transfer* **119**, 366–370.

Qiao, Z. & Kaloni, P. N. 1998 Non-linear convection in a porous medium with inclined temperature. *Intl J. Heat Mass Transfer* **41**, 2549–2552.

Sarkar, A. & Phillips, O. M. 1992 Effects of horizontal gradients on thermohaline instabilities in a thick porous layer. Phys. Fluids A **4**, 1165–1175.

Thorpe, S. A., Hutt, P. K. & Soulsby, R. 1973 The effect of horizontal gradients on thermohaline convection. *J. Fluid Mech.* **38**, 375–400.

Weber, J. E. 1973 On thermal convection between non-uniformly heated plates. *Intl J. Heat Mass Transfer*. **16**, 961–970.

Weber, J. E. 1974 Convection in a porous medium with horizontal and vertical temperature gradients. *Intl J. Heat Mass Transfer* **17**, 241–248.

Zimmermann, G., Muller, U. & Davis, S. H. 1992 Bénard convection in binary mixtures with Soret effects and solidification. *J. Fluid Mech.* **238**, 657–682.